DELPHI 97-99 CONF 81
28 July, 1997

First Observation of the B^* Dalitz Decay $B^* \to Be^+e^-$

Preliminary

DELPHI Collaboration

M. Feindt, W. Oberschulte gen. Beckmann
University of Karlsruhe
O. Podobrin
CERN-PPE

Abstract

Exploiting the DELPHI silicon microvertex detector of the years 1994 to track very low energy electrons and using an inclusive B reconstruction method, the second order electromagnetic (Dalitz-) decay $B^* \to Be^+e^-$ has been observed for the first time. The ratio $\Gamma(B^* \to Be^+e^-)/\Gamma(B^* \to B\gamma)$ is determined to be in agreement with the QED expectation.

Paper submitted to the LP'97 Conference
Hamburg, July 28 - August 1st

1 Introduction

In e^+e^-collisions at the Large Electron-Positron (LEP) collider at CERN, with centre-of-mass energies close to the Z^0 mass of 91.2 GeV, the copious production of $b\bar{b}$ events has recently revealed many new results on B meson spectroscopy. Using inclusive B reconstruction methods, the decays $\mathrm{B}^* \to \mathrm{B}\gamma$ [1, 2, 3, 5] and $\mathrm{B}^{**} \to \mathrm{B}\pi$ [6, 7, 3] have been clearly established, and evidence for $\mathrm{B}_{s1} \to BK$ [6, 7] and $\mathrm{B}^*_{s2} \to B^*K$ [7] as well as Σ_b and $\Sigma^*_b \to \Lambda_b\pi$ [8] has been found. $75 \pm 4\%$ of all B mesons at LEP are measured to be decay products of the B^* [9]. Because the mass difference between the B^* and ground state B mesons is just 45.7 ± 0.4 MeV/c^2 [10], strong decays are kinematically forbidden, and the electromagnetic M1 transition $\mathrm{B}^* \to \mathrm{B}\gamma$ is the dominating decay mode. Another kinematically allowed decay mode is the second order electromagnetic decay $\mathrm{B}^* \to \mathrm{B}e^+e^-$, with an expected branching ratio in the order of half a percent. Similar to the decay $\pi^0 \to \gamma e^+e^-$, first predicted by R. H. Dalitz [11], this decay is called B^* Dalitz decay. The large number of inclusively reconstructed B-mesons at DELPHI and the large B^* cross section allow one to search for this rare decay mode.

Although the B fragmentation is hard [12], the mean B^* photon energy in the laboratory frame at LEP 1 is only about 300 MeV, with an upper limit of just 800 MeV. For this reason DELPHI, ALEPH and OPAL have used converted photons for the B^* studies. The energies of electron and positron are much smaller, the average momentum is less than 160 MeV/c for each lepton. Both are not well measured with the track chambers of the DELPHI detector. Because of their curvature in the magnetic field, these particles do not reach the usual track chambers and are confined to the vertex detector region. The DELPHI vertex detector in the configuration of the year 1994, allowed tracks to be reconstructed in three dimensions. Using a new algorithm, it was possible to reconstruct the low momentum tracks of electron and positron, from points in the vertex detector alone.

The B meson four momentum was estimated from the momentum sum of the decay particles of the B meson. With this inclusive technique the mass difference distribution of $\Delta M = M(\mathrm{B}e^+e^-) - M(\mathrm{B})$ was measured to look for the B^* Dalitz decay. The result can be compared with a precise prediction of Quantum Electrodynamics.

2 The B^* Dalitz Decay

Analogous to the π^0 meson the B^* meson can decay into B e^+e^-. The photon could with a small probability be emitted off shell with a finite q^2 value and decay into an e^+e^-pair. This internal conversion decay is governed by the amplitude [13] :

$$\mathcal{M} = 4\pi\alpha i[f_{B^*B}(q^2)\varepsilon^{\alpha\beta\gamma\delta}p_\alpha q_\beta \epsilon_\gamma] \cdot \frac{1}{q^2} \cdot [\bar{u}\gamma_\delta u] \ , \tag{1}$$

with p_α and q_β being the four-momenta of the B and the virtual photon in the B^* centre–of–mass system, ϵ_γ the B^* polarisation vector, u and $\bar{u}$ the electron and positron's spinors, $1/q^2$ the virtual photon propagator and $f_{B^*B}(q^2)$ the B^*–B transition form factor. The effective mass spectrum derived from this amplitude is:

$$\frac{\mathrm{d}\Gamma(B^* \to Be^+e^-)}{\mathrm{d}q^2 \cdot \Gamma(B^* \to B\gamma)} = \frac{\alpha}{3\pi}\left[1-\frac{4m_e^2}{q^2}\right]^{1/2}\left[1+\frac{2m_e^2}{q^2}\right]\frac{1}{q^2} \cdot \left[\left(1+\frac{q^2}{m_{B^*}^2-m_B^2}\right)^2-\frac{4m_{B^*}^2 q^2}{(m_{B^*}^2-m_B^2)^2}\right]^{3/2} F_{B^*B}^2(q^2)\ . \tag{2}$$

$F_{B^*B}(q^2) = f_{B^*B}(q^2)/f_{B^*B}(0)$ is the normalised transition form factor with $F_{B^*B}(0) = 1$, describing hadronic corrections. The function used for the form factor depends on particular dynamical models. A typical ansatz is linear :

$$F(q^2) = 1 + 1/6 \cdot \langle r_{B^*B}^2\rangle q^2, \tag{3}$$

where $\langle r_{B^*B}^2\rangle$ is interpreted as mean square size of the interaction region. As can be found in [14], a value of :

$$\langle r_{B^*B}\rangle = 0.6 \text{ fm} \tag{4}$$

is reasonable for a meson. Another model uses the pole form :

$$F(q^2) = \frac{1}{1-q^2/\Lambda^2}\ . \tag{5}$$

In the Vector Meson Dominance model the pole mass Λ is related to virtual vector meson masses (m_ρ, m_ω etc.), depending on the flavour wave function of initial and final mesons (see [14]). For the transition B*–B a resonance of Υ could be possible, but more suppressed, compared to lighter mesons.

All approaches should not differ too much since the maximum q-value of the B*–B splitting is quite low. In fact only a maximum deviation of 10^{-2} from unity is observed in this q^2region. The integral is clearly dominated from the decrease in the first part of the spectrum eq.(2). The integration boundaries are:

$$2m_e \leq q \leq \Delta m(\mathrm{B}^* - \mathrm{B})\ . \tag{6}$$

Using $m_B = 5278.9 \pm 1.8$ MeV/c^2 [10] and $\Delta m(\mathrm{B}^* - \mathrm{B}) = 45.7 \pm 0.4$ MeV/c^2 from [10] the integration of formula (2) gives:

$$\frac{\Gamma(\mathrm{B}^* \to \mathrm{B}e^+e^-)}{\Gamma(\mathrm{B}^* \to \mathrm{B}\gamma)} = (4.657 \pm 0.013) \times 10^{-3} \tag{7}$$

in point-like QED, i.e. a constant transition form factor equal to 1.
Other models give:

finite size model		
with $\langle r_{B^*B}\rangle = 1$ fm	:	$(4.659 \pm 0.013) \times 10^{-3}$
ρ–VDM, $m_\rho = 0.767\mathrm{GeV}/c^2$	:	$(4.658 \pm 0.013) \times 10^{-3}$
Υ–VDM, $m_\Upsilon = 9.460\mathrm{GeV}/c^2$	:	$(4.656 \pm 0.013) \times 10^{-3}$

As a consequence of the small available q^2 range in the B* decay, different values for $\langle r^2\rangle$ or Λ^2 have only a very minor effect on the q^2 spectrum and the integrated branching ratio. The error is dominated by the experimental uncertainty on the B*–B mass difference. Thus there is a very precise theoretical prediction to test with the B* Dalitz decays.

3 Dalitz photon reconstruction

A complete description of the DELPHI detector can be found in reference [15], and performance figures are summarized in [16]. The detectors most relevant to this study are the inner tracking chambers (Vertex Detector (VD), Inner Detector and Time Projection Chamber (TPC)). The DELPHI vertex detector consists of three concentric cylindrical shells of Si-strip detectors at radii of 6.3, 9 and 11 cm parallel to the beam-pipe for precision reconstruction near the interaction region. The inner- and outermost layer of the vertex detector in addition provide an accurate measurement of the z-coordinate (along the beam direction).

In order to enhance the efficiency for very low energy electrons from the main vertex, an algorithm was developed to reconstruct strongly curved tracks from non-associated vertex detector hits (in the following called "VD tracks"). Using this algorithm after the normal tracking, finds many tracks which are measured only by the vertex detector, in the average 0.6 per event. These tracks are usually lost in cracks of the other tracking devices, interact with the material between VD and TPC or are too low energy to be measured. Starting from the outermost VD layer, free hits are collected in the other two layers to form a track in the R-ϕ [1] projection. By accepting only tracks with hits in all three layers and requiring reasonable values for the impact parameter, the procedure ends up with trustworthy candidates, see e.g. [17, 18] , where decaying $\Sigma^- \to n\pi^-$ baryons have been reconstructed using these new tracks. The algorithm is efficient down to transverse momenta of 30 MeV. When a unique solution is found, also the z-coordinate at the perigee and the polar angle θ, to the beam direction, can be determined; otherwise only a rough θ-value can be estimated from the module geometry.

To calculate the dE/dx of a track in the vertex detector the associated hits are taken and the signal values are kept. After the path length correction and signal calibration, a maximum likelihood fit is applied and the Landau peak position can be calculated. For tracks with more than two hits the resulting dE/dx is shown in fig. 1, for the whole possible momentum range of hadronic Z^0-decays. In this distribution several bands are visible, which allow a separation or particle identification. The resolution depends on the number of associated hits, being 15%/(mips) for three or more hits. The VD tracks have by definition at least three hits in the vertex detector and this guarantees a reliable dE/dx measurement. They allow one to explore the low momentum part of fig.1 with a particle identification below 100 MeV/c.

To search for Dalitz photons, a loop over pairs of two oppositely charged tracks is performed. In case a dE/dx measurement in the TPC is available, it must be consistent with the electron hypothesis. For the VD tracks a track fit is applied using the electron mass for the dE/dx correction. Additionally the measured specific ionisation (dE/dx) in the vertex detector is required to be less 1.5/(mips), to enrich electrons.

Since the B*-decay is taking place at the primary vertex, the pair is required to form a vertex compatible with the event primary vertex. Therefore the impact parameter to

[1] In the DELPHI frame R is $\sqrt{x^2+y^2}$ and ϕ the azimuth angle, with z along the beam direction.

the primary vertex in R-ϕ is required to be less than 0.2 cm. The primary vertex in a b-event is estimated following the method described below. First a primary vertex fit is performed. The measured beam spot position and size also enter the fit. Starting from all well measured tracks with at least two measurements in the vertex detector, the tracks contributing the largest χ^2 are successively removed, until an acceptable probability is reached.

Fig. 2 shows the resulting $q^2 = m^2_{e^+e^-}$ spectrum of the accepted pairs with low opening angle ($\cos\alpha_{e^+e^-} > 0.75$). A clear enhancement due to internal photon conversions is visible at very low q^2 values. In the following all e^+e^-pairs with a q^2 of less than $5{\times}10^{-5}$ GeV^2 are called "virtual photons". The large amount of available π^0 decays in multihadronic events is a good test ground for efficiency and purity of the Dalitz photon reconstructions. The four momentum vectors of tracks can be compared after reconstruction with Monte Carlo simulation level. Picking up the final electron positron pair on generator level and the corresponding tracks on the Monte Carlo simulation gives the momentum vector of the Dalitz photon. The background and efficiency of the Dalitz pair selection can be calculated from comparison with simulation. For the total efficiency one gets about $\epsilon = 0.121 \pm 0.015$ with a purity of $P = 0.747 \pm 0.012$. Background of real photons converted at the beam pipe is heavily suppressed, by the hard requirements on the impact parameter an the primary vertex fit. Especially low energy converted photons will fail these requirements. Only a fraction of 0.6% was found after the cuts and a fraction of 1.17 % in the whole sample of Dalitz pairs. Combining the four-vectors of these photons with well-measured converted photons [2, 19] leads to the invariant mass spectrum shown in Fig.3, exhibiting a clear peak due to $\pi^0 \to \gamma e^+e^-$ decays.

4 B Meson Reconstruction

The algorithm that is used to enhance the $b\bar{b}$ content relies on good vertex measurements. Therefore the analysis is restricted to the barrel region ($45^\circ < \theta < 135^\circ$), where there is complete vertex detector coverage. The impact parameters of charged tracks with respect to the primary vertex which is fitted on an event by event basis are taken. The output is a probability, of a selected sample of tracks coming from the primary vertex. To select $b\bar{b}$ events low values of this probability are required. This method is described in detail in [20]. It was run at a working point providing an efficiency of (72 ± 3) % and a purity of (75 ± 4) % for $b\bar{b}$ events. This beauty-enhanced sample consists of about 276,800 events.

The B mesons are reconstructed in an inclusive fashion with the so-called rapidity algorithm, as applied and described in detail in the DELPHI B* paper [2]. This works by collecting all particles with a rapidity $y = 1/2 \log\frac{E+p_z}{E-p_z}$ relative to the thrust axis above 1.5 units, assuming to be B decay products. The four momenta of these particles are added together in each hemisphere, leading to an energy E_y and mass m_y for the B meson. The requirements for a B four momentum reconstruction are : $E_y > 20$ GeV, $|m_y - 4.8| < 2.5\text{GeV}/c^2$ and $x_h = E_{hem}/E_{beam}$ with $0.6 < x_h > 1.1$.

The energy precision is 7% for 75% of the B mesons, the remainder constituting a non-Gaussian tail towards higher energies. The angular resolution in θ and ϕ can be parameterized as double Gaussian with widths of 15 mrad for 60% of the data and

38 mrad for the remaining 40%. The virtual photons are combined with inclusively reconstructed B-mesons. The mass difference spectrum of $\Delta M = M(Be^+e^-) - M(B)$ is shown in Fig.4. It shows clear evidence for the decay $B^* \to Be^+e^-$.

The background is estimated using normal $q\bar{q}$ simulated events, including the B^*-rate of 0.65 per b-quark, to check whether converted photons from the $B^* \to B\gamma$ decay can contribute to the Dalitz decay signal. With the cuts on q^2 and the R-ϕ impact parameter this is nearly completely prevented. This background is flat in the interesting signal region of $0.01 - 0.08$ GeV and in the order of 1.8 entries per bin. The main background source is due to π^0 Dalitz photons and combinatorial background of two charged tracks giving also small q^2. The shape predicted from the Monte Carlo simulation is fitted to the formula:

$$B(x) = a_1[(x - 0.01)(a_4 - x)]^{a_2} \exp[-a_3(x - \frac{1}{2}(0.01 + a_4))]$$

and used as a background model for the data. In addition to the background a signal shape from simulation studies is fitted yielding 74±17 events in the peak, with a reconstructed mass difference of 44±1.3 MeV/c^2, in good agreement with the world average. The width was found to be 11 ± 1.9 MeV/c^2 as expected, since it is dominated by the angular resolution of the inclusive B reconstruction [2].

4.1 Efficiency

Taking 9194 simulated $B^* \to Be^+e^-$ decays in a sample of 7377 $b\bar{b}$ events allows a calculation of the efficiency after event selection, b-quark tagging and Dalitz pair requirements. This simulation sample was processed with the same tracking software as the data. The measured mass difference distribution in the simulation was fitted with a double Gaussian, giving a resolution of 7.0 MeV/c^2 for 90% and 14.0 MeV/c for 10% of the signal remainder. The resolution is dominated by the angular resolution of the inclusive B reconstruction. The selected number of entries in the mass region of 0.02–0.07 GeV/c^2 gives a total efficiency of:

$$\epsilon = 0.0471 \pm 0.0022(\text{stat.}) \pm 0.0026(\text{syst.}). \quad (8)$$

The acceptance is influenced by the dE/dx determination, the choice of signal region and Dalitz efficiency. The b-quark tagging efficiency uncertainty is assumed to have a minor effect. The dominant influence in the efficiency is the Dalitz pair efficiency itself. A difference in the efficiency is expected as the vertex detector efficiency has to be corrected by tables, tuned with tracks higher in momentum than the Dalitz pairs. Also the average number of VD tracks in data and simulation samples is different. To check whether the efficiency is different in the simulation sample, the total number of Dalitz photons per event in the energy region less than 2 GeV in simulation and data can be taken. This motivates a correction to the prior efficiency of expression (8) with factor of $\mathcal{C} = 0.871 \pm 0.087$:

$$\epsilon(\text{B}e^+e^-) = \epsilon \cdot \mathcal{C} \ .$$

Including the uncertainty of the π^0 production this ends in the total efficiency for the B^* Dalitz decay of:

$$\epsilon(\text{B}e^+e^-) = 0.0410 \pm 0.0051(\text{syst.}) \ . \quad (9)$$

The systematic error is dominated by the efficiency correction, all contributions have been added in quadrature.

4.2 Calculation of the Cross Section

The Observation of the B* Dalitz decay allows the measurement of the inclusive cross section, which can be calculated from the number of measured decays per b quark hemisphere:

$$\frac{\sigma(\mathrm{B}^* \to \mathrm{B}e^+e^-)}{\sigma_{b-quark}} = \frac{N(\mathrm{B}^*)/\epsilon(\mathrm{B}e^+e^-)}{2 \cdot N(b\bar{b})/\epsilon_{b\bar{b}} \cdot P_{b\bar{b}}} \cdot \tag{10}$$

The impact parameter tagging using an event probability cut of $\mathcal{P}_E^+ < 0.01$ gives a sample of 276800 $b\bar{b}$events. The efficiency and purity of this selection cut are taken from [20], i.e. $\epsilon_{b\bar{b}} = 0.72$ and $P_{b\bar{b}} = 0.75$. Together with 74 ± 17(stat.) signal entries and the total efficiency $\epsilon(\mathrm{B}e^+e^-)$=0.041 one gets:

$$\frac{\sigma(\mathrm{B}^* \to \mathrm{B}e^+e^-)}{\sigma_{b-quark}} = (3.21 \pm 0.62(\mathrm{stat.})) \times 10^{-3} , \tag{11}$$

for the inclusive cross section.

The ratio of the decay widths as predicted in chapter 1 can be evaluated by dividing this result with the production cross section of the usual B* decay in b-quark events, as given in table [9] (LEP average) $\sigma(\mathrm{B}^*)/\sigma_{b-quark} = 0.67 \pm 0.03$,

$$\frac{\Gamma(\mathrm{B}^* \to \mathrm{B}e^+e^-)}{\Gamma(\mathrm{B}^* \to \mathrm{B}\gamma)} = (4.79 \pm 0.95(\mathrm{stat.}) \pm 0.21(\mathrm{B}\gamma\text{-rate})) \times 10^{-3} . \tag{12}$$

4.2.1 Systematic Uncertainties

The systematic influences on the measured cross section (see eq.(11)) are expected to come mostly from the efficiency calculation and the signal determination. The sources for these uncertainties have been discussed above. Other sources are the b-quark tagging purity and efficiency errors, taken from [20]. Additionally the cuts on $|\cos\Theta_{Thrust}|$, the B meson energy E_y, and the rapidity mass $|4.8 - m_y|$ and the b-quark tagging probability have been varied in a reasonable range. The variation was found to be below 6% of the final result. The contributions to the uncertainty are listed below: For the total efficiency $\epsilon(\mathrm{B}e^+e^-)$ statistical and systematic errors have been added in quadrature. The relative uncertainty on the number of signal entries is expected to be reduced when a smooth mass difference distribution with enough statistics in data and simulation is available.

Adding up all these contribution in quadrature gives the total systematic error on the production cross section : 0.59×10^{-3} of $\mathrm{B}^* \to \mathrm{B}e^+e^-$ in b-quark events.

5 Results

Using the 1994 data collected with the DELPHI detector at LEP, a sample of 1.4 million multi–hadronic events was collected. With the impact parameter tagging and the inclusive B meson reconstruction shown in chapter 5 four vectors of B mesons can be reconstructed. The combination of these B mesons with the Dalitz pairs explained in the previous chapter show a peak in the mass difference distribution $\Delta M = M(\mathrm{B}e^+e^-) - M(\mathrm{B})$. Using simulation samples for signal and background shape, 74 ± 17 signal entries can be extracted and the total efficiency to reconstruct B* Dalitz decays is computed to be 4%. The background from simulation is found to be smooth and agrees well with the data. Taking the uncertainties from table 1 into account and adding the contributions in quadrature one gets for the inclusive cross section:

$$\frac{\sigma(\mathrm{B}^* \to \mathrm{B}e^+e^-)}{\sigma_{b-quark}} = (3.21 \pm 0.62(\mathrm{stat.}) \pm 0.59(\mathrm{syst.})) \times 10^{-3}\ . \qquad (13)$$

This corresponds to a decay width ratio of:

$$\frac{\Gamma(\mathrm{B}^* \to \mathrm{B}e^+e^-)}{\Gamma(\mathrm{B}^* \to \mathrm{B}\gamma)} = (4.79 \pm 0.93(\mathrm{stat.}) \pm 0.91(\mathrm{syst.})) \times 10^{-3}\ . \qquad (14)$$

The measured ratio agrees with the expected rate of 4.7×10^{-3} from Quantum Electrodynamics and confirms the observation of the second order M1 electromagnetic decay of the vector meson B* into a pseudoscalar B meson.

The statistical error could be reduced with more collected data. Also the systematic error would decrease, when more statistics in data and simulation sample give a smooth mass difference distribution with less fluctuations.

The dominant contribution to the systematic error comes from the uncertainty of the Dalitz pair efficiency. The efficiency is found to be different in the simulation sample.

Table 1: The systematic contribution to the relative cross section.

variable	value ± error	error in cross section $\sigma(\mathrm{B}e^+e^-)/\sigma(b-quarks)$
$\epsilon(\mathrm{B}e^+e^-)$	0.0410 ± 0.0051	0.394×10^{-3}
N_{B^*}	74 ± 8	0.347×10^{-3}
$\epsilon_{b\bar{b}}$	0.72 ± 0.03	0.132×10^{-3}
$P_{b\bar{b}}$	0.75 ± 0.04	0.169×10^{-3}
cuts		0.156×10^{-3}
total		0.588×10^{-3}

References

[1] L3 Coll., M. Acciarri et al., *Phys. Lett.* **B 345** *(1995) 589.*

[2] DELPHI Coll., P. Abreu et al., *Z. Phys.* **C 68** *(1995) 353.*

[3] ALEPH Coll., D. Busculic et al., *Z. Phys.* **C 69** *(1996) 393.*

[4] L3 Coll. L3 *unnumberd contr.paper to EPS 1995 Bruxelles.*

[5] OPAL Coll. OPAL *physics note pn-231, contr. paper to ICHEP 1996 Warsaw pa05-037.*

[6] R. Akers et al. OPAL Coll. *Z. Phys.* **C 66** *(1995) 19.*

[7] C. Kreuter O. Podobrin DELPHI Coll., M. Feindt. *DELPHI-95-105, contribution eps0563 to the Brussels EPS Conference, 1995.*

[8] A. Miagkov O. Podobrin DELPHI Coll. M. Feindt, C. Kreuter. *DELPHI-95-107, contribution eps0565 to the Brussels EPS Conference, 1995.*

[9] M. Feindt. *CERN-PPE/95-139, Procs. Hadron '95, Manchester, World Scientific 1995, p. 84.*

[10] Review of Particle Properties. *Phys. Rev.* **D 54** *(1996) 1.*

[11] R. H. Dalitz. *Proc. Phys. Doc.(London)* **A 64** *(1951) 667.*

[12] DELPHI Coll., *contr. paper to EPS 1995 Bruxelles, EPS0560,* DELPHI-*Note 95-103 PHYS 538;*
ALEPH Coll., *CERN PPE/95-113 Phys. Lett.* **B 357** *(1995) 699.*

[13] L. G. Landsberg. *Phys. Rep.* **128** *(1985) 301, page 336.*

[14] CELLO Coll., H. J. Beherend et al., *Z. Phys.* **C 49** *(1991) 401.*

[15] DELPHI Coll., P. Aariano et al., *CERN-PPE/90-128, Nucl. Instr. Meth.* **A 303** *(1991) 233.*

[16] DELPHI Coll., P. Abreu et al., *CERN-PPE/95-194, Nucl. Instr. Meth.* **A 378** *(1996) 57.*

[17] C. Weiser and M. Feindt. DELPHI *note 96-69 CONF 3, contr. paper to ICHEP 1996 Warsaw pa01-040.*

[18] W. Oberschulte-Beckmann. *Ph.D. thesis University of Karlsruhe IEKP/KA–97-06.*

[19] M. Wielers, *Ph.D. thesis 1995 University of Karlsruhe, IEKP-KA/95-9;*
DELPHI Coll.,W. Adam et al., *Z. Phys.* **C 69** *(1996) 561.*

[20] G. V. Borisov, DELPHI *note 94-125 PROG 208 ;*
G. V. Borisov and C. Mariotti, DELPHI *note 95-142 PHYS 567.*

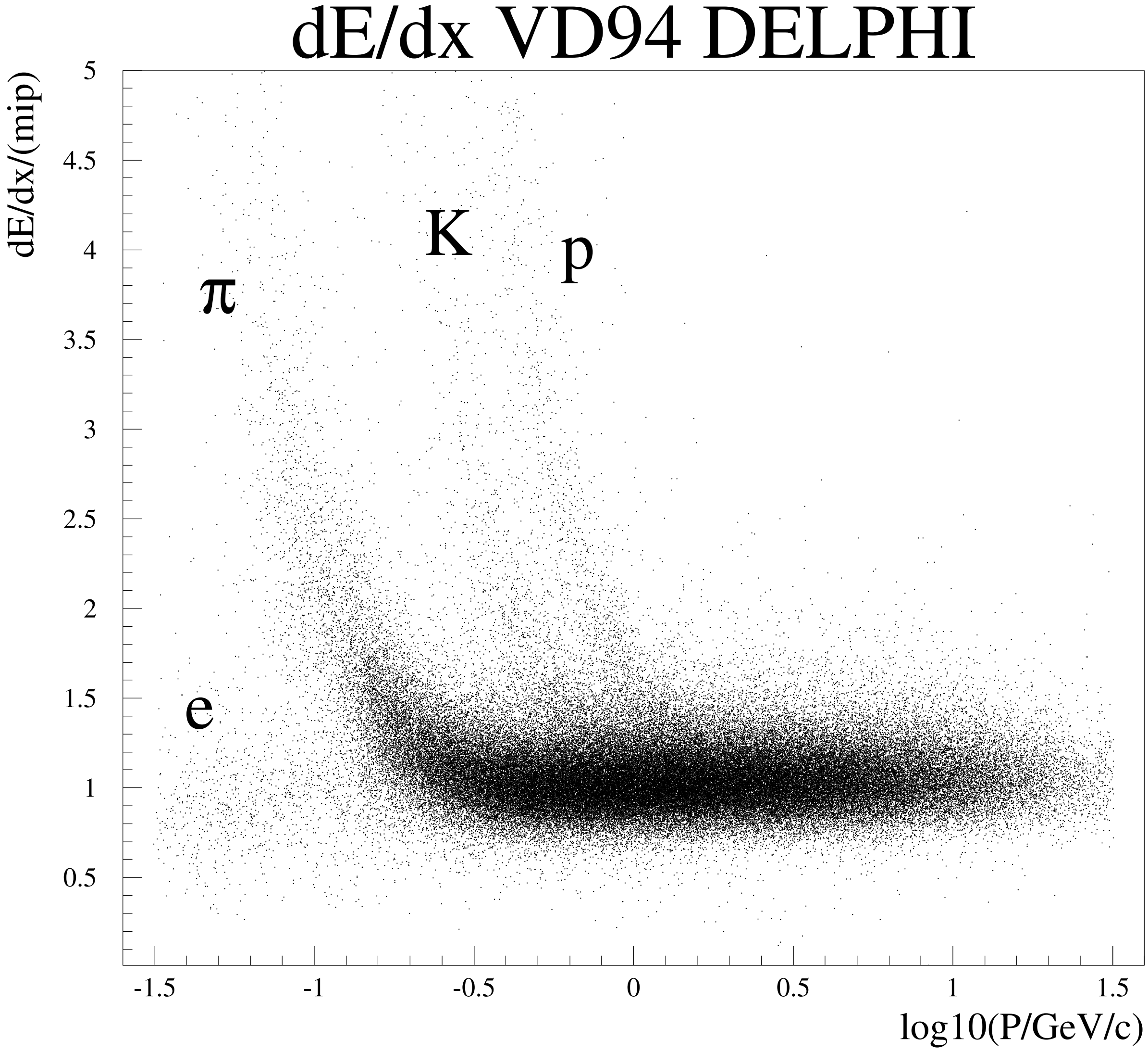

Figure 1: The vertex detector detector dE/dx with three hits and more for the whole momentum range, measured with the 94 vertex detector. Clearly visible are the $e^{\pm}$,$\pi^{\pm}$,Kaon and proton bands. The VD tracks cover the momentum range below 100 MeV/c and show a nice electron/π separation.

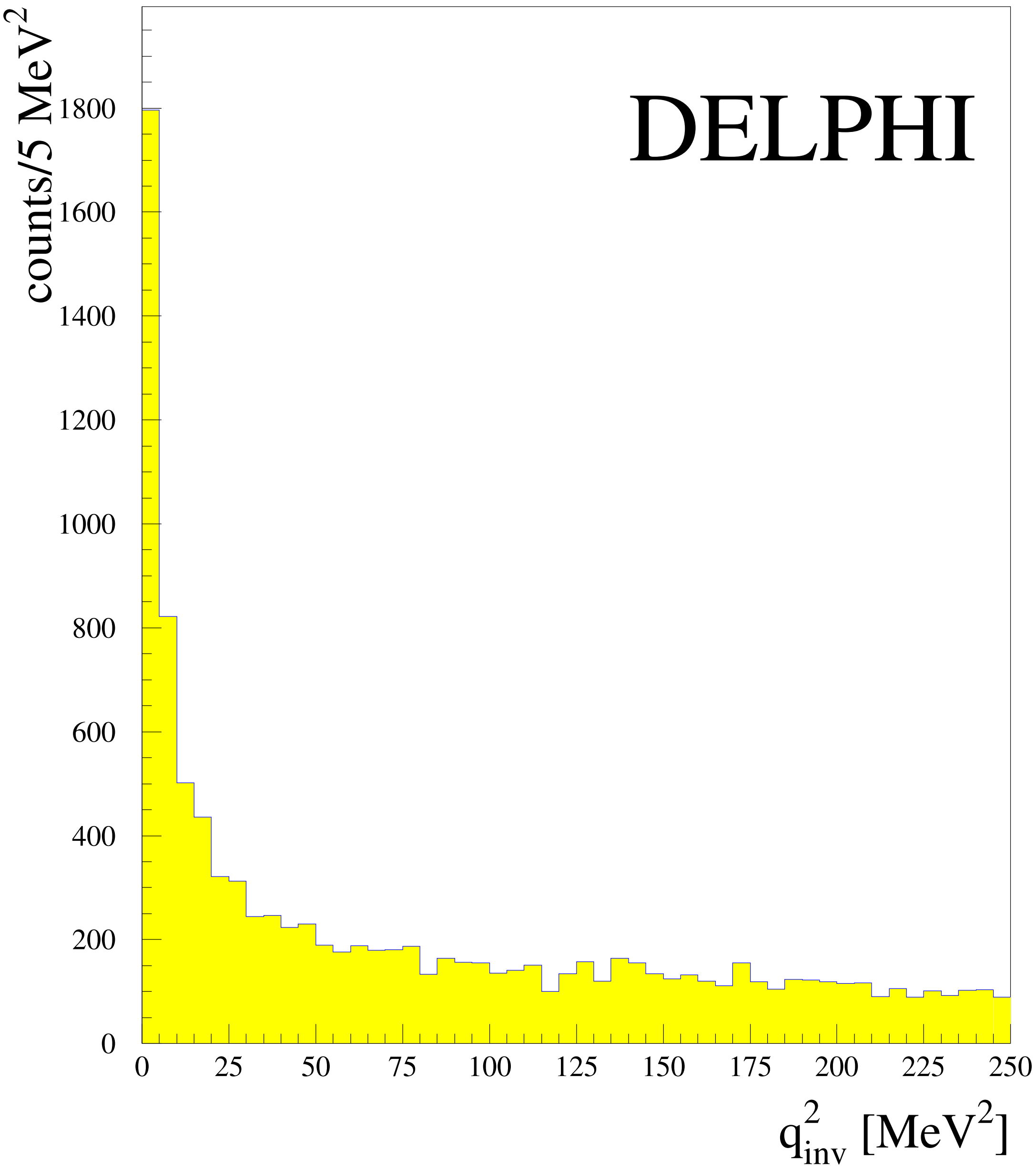

Figure 2: q^2 spectrum of oppositely charged electron candidate tracks. The low q^2 enhancement is due to Dalitz decays, mostly from $\pi^0 s$.

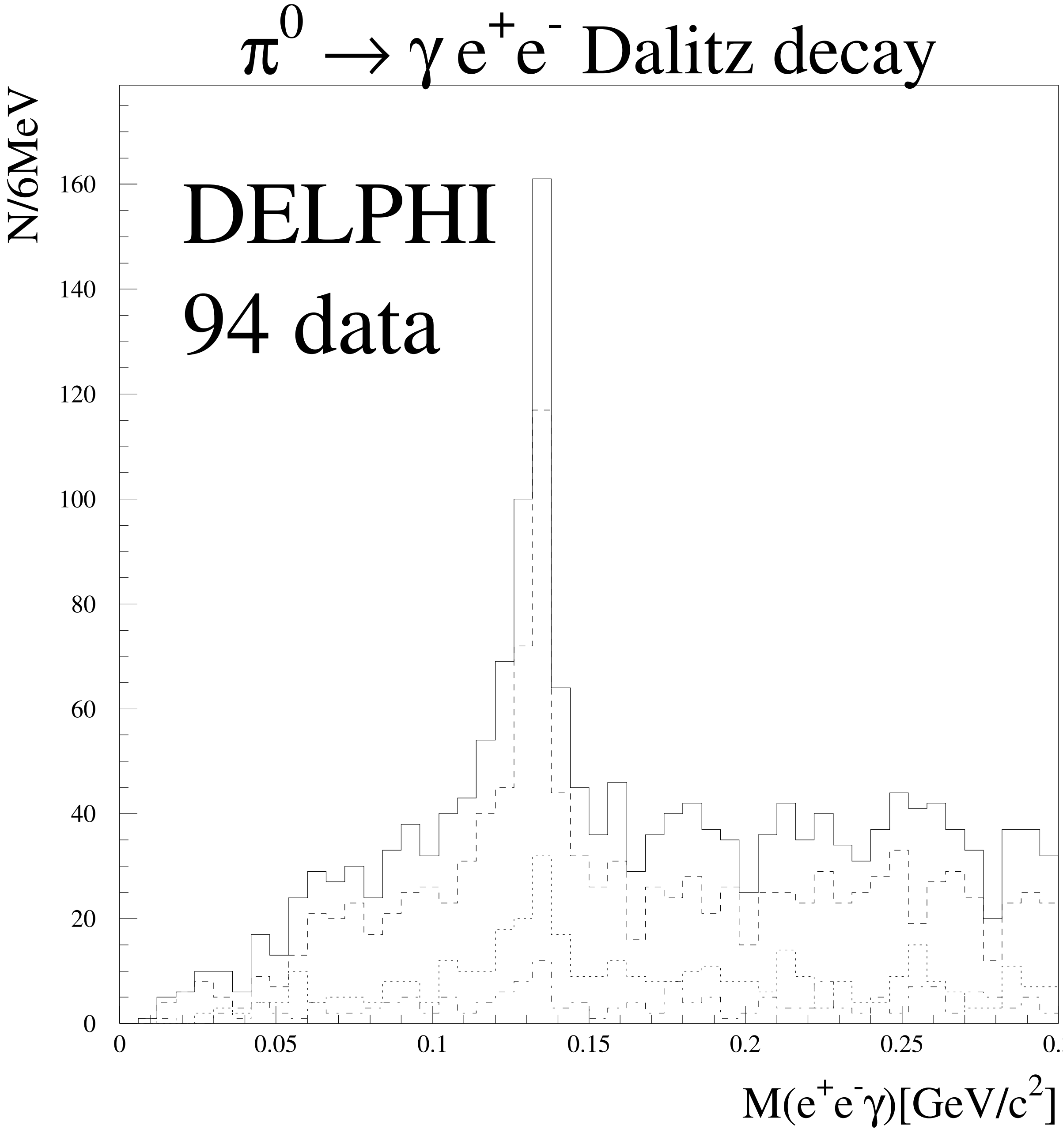

Figure 3: Observation of π^0 Dalitz decay: The invariant mass of one converted photon and one Dalitz photon is shown. The solid line contains all classes of photons, the broken line represents a pair of two TPC tracks, the dotted line a pair of one TPC and one VD-track, the broken dotted line a pair of two VD-tracks.

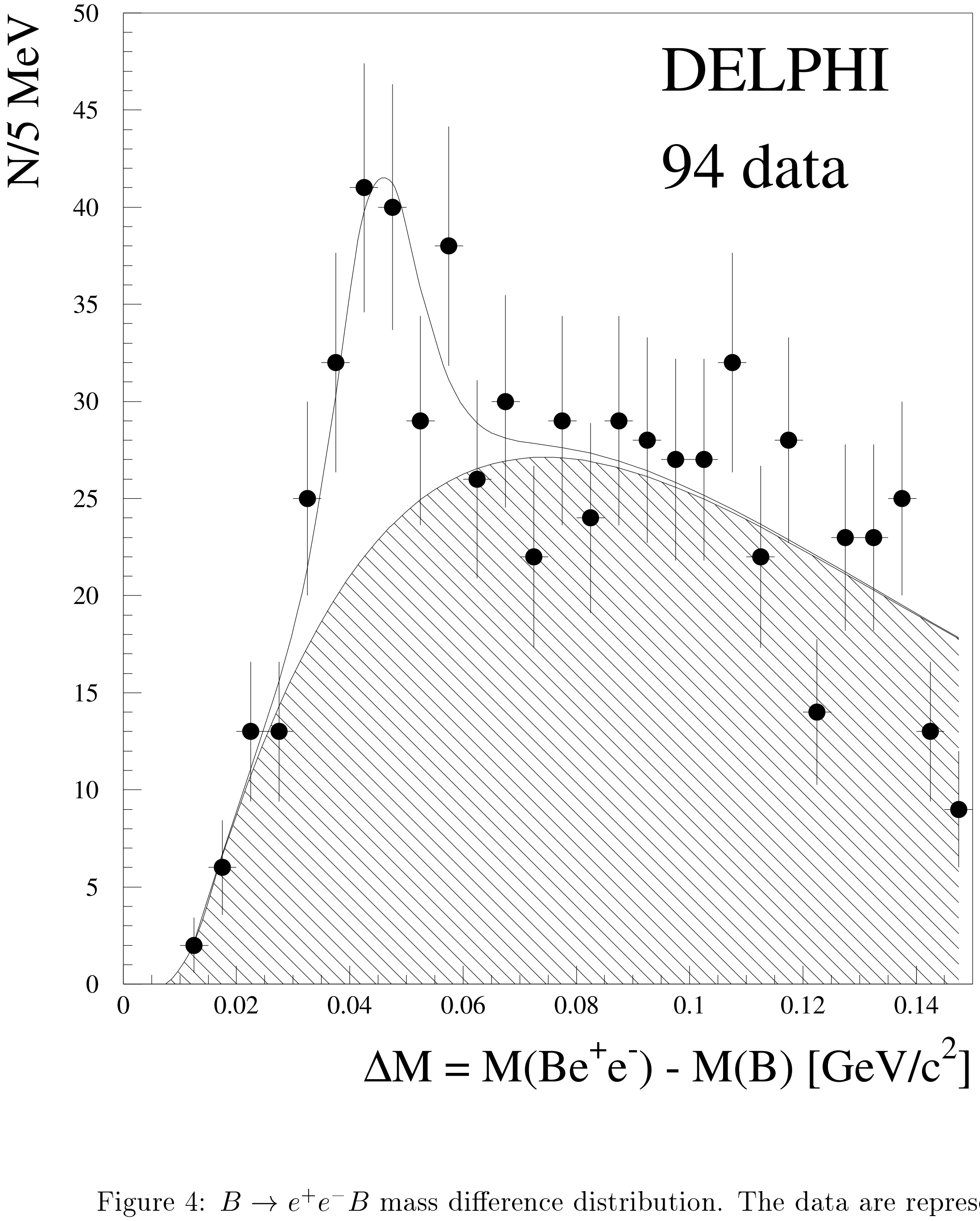

Figure 4: $B \to e^+e^-B$ mass difference distribution. The data are represented by points, the line corresponds to the fit result using background (shaded) and signal shapes predicted by simulation.